INDERSCIENCE PUBLISHERS
Linking academia, business and industry through research

International Journal of Mining and Mineral Engineering

ISSN online: 1754-8918 - ISSN print: 1754-890X
https://www.inderscience.com/ijmme

Machine learning tool to minimise and predict airblast during blasting and to optimise the design of blasting operations

Onalethata Saubi, Rodrigo S. Jamisola Junior, Raymond S. Suglo, Oduetse Matsebe

DOI: 10.1504/IJMME.2025.10070547

Article History:

Received:	04 October 2024
Last revised:	06 February 2025
Accepted:	13 February 2025
Published online:	23 June 2025

Copyright © 2025 Inderscience Enterprises Ltd.

Machine learning tool to minimise and predict airblast during blasting and to optimise the design of blasting operations

Onalethata Saubi*

Department of Mining Engineering,
Botswana International University of Science and Technology,
Palapye, Botswana
Email: onalethata.saubi@studentmail.biust.ac.bw
Email: SO13000604@biust.ac.bw
*Corresponding author

Rodrigo S. Jamisola Junior

Department of Mechanical, Energy and Industrial Engineering,
Botswana International University of Science and Technology,
Palapye, Botswana
Email: jamisolar@biust.ac.bw

Raymond S. Suglo

Department of Mining Engineering,
Botswana International University of Science and Technology,
Palapye, Botswana
Email: suglor@biust.ac.bw

Oduetse Matsebe

Department of Mechanical, Energy and Industrial Engineering,
Botswana International University of Science and Technology,
Palapye, Botswana
Email: matsebeo@biust.ac.bw

Abstract: We present a method to minimise and predict airblast in blasting operations in an open-pit Debswana diamond mine. Blast engineers can use this tool to optimise their blast design to achieve desired blasting operation effect, i.e., airblast. The major novelty of this study is on the creation of a nine-dimensional solution space, optimisation of the blast design parameters, and minimisation of airblast using gradient descent method. We develop a solution surface using artificial neural network (ANN). This is our best-performing machine learning model compared to the three other models used, namely, support vector machine (SVM), k-nearest neighbour (k-NN), and random forest (RF). The computed nine-dimensional solution space has eight input parameters: stemming, distance from the blast face to

Copyright © The Author(s) 2025. Published by Inderscience Publishers Ltd. This is an Open Access Article distributed under the CC BY-NC-ND license. (http://creativecommons.org/licenses/by/4.0/)

the monitoring point, burden, powder factor, hole diameter, maximum charge per delay, spacing, and hole depth. Sensitivity analysis revealed that stemming is the most sensitive input parameter while spacing is the least sensitive. The minimum value of airblast computed in this study through unconstrained optimisation is around 40 dB, which is approximately equivalent to the sound of a whisper. This framework is adaptable to various geological and operational settings, highlighting its broader applicability in improving environmental compliance and blasting efficiency.

Keywords: airblast; machine learning; blast design; optimisation; sensitivity analysis; open-pit diamond mine.

Reference to this paper should be made as follows: Saubi, O., Jamisola Jr., R.S., Suglo, R.S. and Matsebe, O. (2025) 'Machine learning tool to minimise and predict airblast during blasting and to optimise the design of blasting operations', *Int. J. Mining and Mineral Engineering*, Vol. 16, No. 2, pp.148–167.

Biographical notes: Onalethata Saubi received his BEng in Mining Engineering from BIUST in 2019 and an MEng in 2023. He is currently pursuing a PhD at BIUST, focusing on AI applications in mining. From 2019 to 2022, he was a teaching assistant and is currently a research assistant on a Debswana-funded project modeling blasting impacts and slope stability using AI. His research interests include AI in drilling, blasting, load and haul, mine ventilation, and planning, as well as geotechnical applications such as slope stability and tunnel performance. He also explores AI-driven modeling, simulation, and optimization of mining operations.

Rodrigo S. Jamisola Junior received his BS in Mechanical Engineering from the University of the Philippines-Diliman in 1993, MEng from the National University of Singapore in 2001, MSc in Electrical and Computer Engineering from Colorado State University in 2006, and PhD in Electronics and Communications Engineering from De La Salle University-Manila in 2009. He was an Assistant Professor at De La Salle University-Manila in 2008. Currently, he is an Associate Professor at the Botswana International University of Science and Technology in Palapye, Botswana. He leads externally funded projects from Debswana Diamond Company and the US Army.

Raymond S. Suglo is a Professor and the Head of the Mining Engineering Department at BIUST, Palapye, Botswana. His research focuses on mine ventilation, safety engineering, mining systems simulation, mine planning, and environmental management. He has 78 publications, including 39 refereed journal papers and two book chapters. He is a registered Professional Engineer with the Engineers Registration Board of Botswana and a member of SME, CIM, and GhIE.

Oduetse Matsebe is a Senior Lecturer and the Head of the Department of Mechanical, Energy and Industrial Engineering at the Botswana International University of Science and Technology (BIUST). His research interests include applying artificial intelligence and machine learning techniques to autonomous robotics, predictive maintenance, control systems, solar tracking systems, and data analytics.

1 Introduction

Blasting is the method of breaking rocks into smaller pieces by using explosives and is widely used in mining and civil engineering as the first stage in processing materials. It is one of the most widely accepted and cost-effective methods for rock fragmentation. However, only a small percentage of the explosive's energy, approximately 20% to 30%, is utilised for rock breaking, while the remaining 70% to 80% contributes to undesirable environmental effects such as flyrock, ground vibration, back-break, and airblast (Yu et al., 2020; Khandelwal and Kankar, 2011; Trivedi et al., 2015; Monjezi and Dehghani, 2008).

Airblast, caused by air over-pressure (AOp), can have detrimental effects on nearby buildings, such as window rattling and damage to roofing materials. It also leads to discomfort and irritation to humans and animals (Sawmliana et al., 2007). The AOp is generated by variations in air density, causing the shock wave from a blast to refract horizontally, dissipating over distance and time. The pressure wave that is produced comprises sounds within the audible range and those below the level of human hearing (Bhandari, 1997). The audible sound corresponds to frequencies greater than 15 hertz in the pressure wave emitted immediately after a blast, while the sub-audible sound lies in the infrasound region with frequencies lower than 15 hertz. Typically, the sub-audible portion is more prominent in regions far from the blast site (Faramarzi et al., 2014).

The AOp is typically measured in terms of pascals and decibels. Numerous factors affect AOp, which can be categorised as either controllable or uncontrollable parameters (Khandelwal and Kankar, 2011; Dindarloo, 2015). Controllable parameters, such as explosives and blast design properties, are man-made, while uncontrollable parameters, including geology, rock mass properties, and atmospheric conditions, are naturally occurring. Among the input parameters influencing AOp, the distance between the blast face and the monitoring point and the maximum charge per delay have been identified as the most influential (Dumakor-Dupey et al., 2021). Researchers have developed a variety of empirical models to predict AOp (Armaghani et al., 2015b; Chen et al., 2022; Siskind et al., 1980; Hustrulid, 1999; Kuzu et al., 2009). One widely used model is the US Bureau of Mines (USBM) formula, which is applied in the absence of monitoring, as expressed by (1) (Siskind et al., 1980; Nguyen and Bui, 2020; Keshtegar et al., 2019; Armaghani et al., 2018).

$$AOp = H * \left(\frac{DI}{MC^{0.33}} \right)^{-\beta} \tag{1}$$

where MC and DI stand for the maximum charge per delay (kg) and distance (m) between the blast face and the monitoring point, respectively. The site-specific constants H and β are deduced by regression analysis through conversion to linear form.

Empirical models have inherent limitations due to their reliance on a limited number of input parameters and their ability to output only one parameter at a time. These models cannot capture the nonlinear relationships between the involved parameters and are site-specific (Singh et al., 2004). This limitation has led to the adoption of artificial intelligence (AI) methods to overcome these challenges. Khandelwal and Kankar (2011) utilised SVM and a generalised predictor equation to predict AOp. The MC and DI were considered as model inputs. The SVM-based predictions closely matched the measured AOp, while the generalised predictor equation showed a high error.

Chen et al. (2022) employed SVM optimised with the grasshopper optimiser (GO) algorithm to predict airblast. The Boruta algorithm (BFS) was used for input selection, and a combined model called SVR-GO-BFS was developed. The findings showed that SVR-GO-BFS achieved the best performance, with a coefficient of determination (R^2) of 0.983 and a root mean square error (RMSE) of 1.332, outperforming other baseline models.

Hosseini et al. (2022b) conducted a study on AOp predictions induced by blasting operations using a dataset from the Anguran Lead-Zinc Mine in Iran, which included 90 blasts. A Z-number reliability and fuzzy cognitive map (FCM)-based uncertainty intelligence method was employed to predict AOp. The reliability input weights were then utilised in back-propagation causality-weighted neural networks (BPCWNNs). This model exhibited superior performance in AOp prediction compared to the back-propagation neural network (BPNN) and the generalised feed-forward neural network (GFFNN).

Nguyen and Bui (2019) employed a robust AI system based on ANN and the RF to predict AOp. An empirical technique was also used for comparison purposes. The results demonstrated that the proposed ANN-RF model outperformed the empirical technique with an RMSE of 0.847 and an R^2 value of 0.985. Several researchers have also utilised AI methods to predict airblast, showing their superiority over statistical and empirical methods in terms of higher accuracy and lower errors (Khandelwal and Singh, 2005; Mohamad et al., 2016; Armaghani et al., 2015b; Nguyen et al., 2020; Le et al., 2019; Armaghani et al., 2016; Mohamad et al., 2012; Temeng et al., 2020; Armaghani et al., 2015a; Mahdiyar et al., 2018; Gaopale et al., 2019). Researchers in other engineering fields have also applied AI methods, demonstrating the capabilities of these algorithms in modelling complex problems with a high degree of accuracy (Armaghani et al., 2023; Cai et al., 2022; Saubi et al., 2023b; Zeng et al., 2021; Abdalla and Salih, 2022; Saubi et al., 2023a; Bakhtavar et al., 2021; Mahmood and Mohammed, 2022; Kaklis et al., 2022; Hosseini et al., 2022c,a).

Although there are many studies in machine learning modelling of blasting, none of them were able to present a solution space based on the created model. This solution space is instrumental in optimising the effects of blasting based on the input parameters. At the same time, it also helps in designing the blast parameters by setting an expected output from the solution space and extracting each corresponding input parameters. In particular, we model the relationship between airblast (Ab) and its input parameters, expressed as:

$$Ab = f(B, S, T, L, D, DI, Lc, Pf) \tag{2}$$

where B = burden, S = spacing, T = stemming, L = hole depth, D = hole diameter, DI= distance from the blast point to the monitoring point, Lc = Linear charge, and Pf = powder factor. While traditional approaches rely on empirical methods to estimate $f()$, our approach leverages machine learning to not only predict airblast but also define a solution space for $f()$, enabling:

- optimisation: finding the minimum airblast through random initial points
- blast design: Setting a desired airblast value and solving for corresponding input parameters or assigning constraints on some parameters and solving for the rest.

Unlike prior studies, which treat $f()$ as a black box, our method provides a transparent and actionable solution space, offering predictive, optimisation, and design capabilities. To the best of our knowledge, no previous work has achieved this. The major motivation of this paper is to develop a machine learning (ML) model from the blasting dataset provided by the Debswana Diamond Mine in Orapa, Botswana. This model will be used to help blast engineers create their blast designs and predict airblast with acceptable accuracy. At the same time, our model will allow blast engineers to come up with a blast design that will minimise airblast. Therefore, the following can be listed as this paper's primary contributions.

- the use of a blasting dataset provided by the Debswana Diamond Company in Botswana consisting of 104 blast events
- the development of machine learning models based on four algorithms with eight input parameters. The models are compared against a statistical method and an empirical method
- creation of a nine-dimensional solution space, optimisation of the blast design parameters, and minimisation of airblast using gradient descent method
- sensitivity analysis to ascertain the relative impact of inputs on airblast is conducted using the network weights of the ANN model as opposed to the usual cosine amplitude method.

The remainder of this paper is organised as follows: Section 2 explains the materials and methods used in this study. Results and discussion are covered in Section 3. The last section details the conclusion.

1.1 Blasting in Orapa diamond mine

A blasting dataset consisting of 104 blasting events was collected from the mine records. The mine is located in Southern Africa, Botswana at the coordinates, latitude $21°18'30''$ S and longitude $25°22'10''$ E, as depicted in Figure 1(a). In this mine, blasting operations employ a staggered pattern. Type A explosives (pentolite boosters) and type B explosives (detonators 15 m and 20 m) are used. Bench height is set at 15 m, and blast holes with diameters of 127 mm, 165 mm, and 250 mm are utilised. Each blast typically consists of 40 to 60 holes per row and 15 to 25 rows. Figure 1(b) provides a schematic diagram of the blast geometry. In-pit material handling of the blasted materials and hauling are carried out using shovels, excavators, and rear dump trucks. The mine's production plan for 2018 aimed to extract approximately 153 million carats from 205 million tons of ore over 15 years.

Figure 1 (a) Orapa mine layout (b) Diagram of blast geometry (see online version for colours)

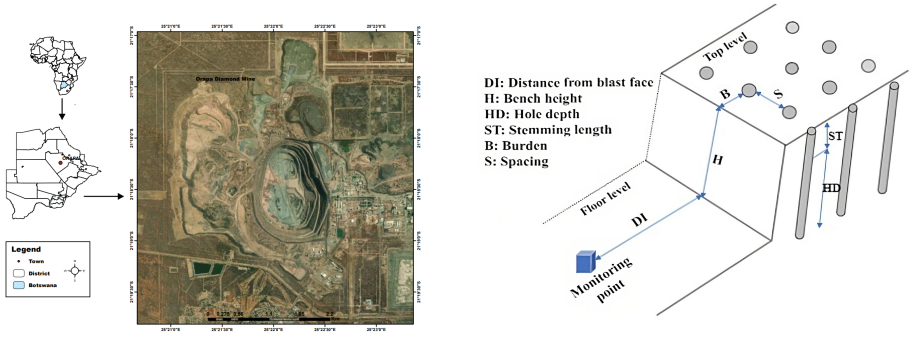

(a) (b)

2 Materials and methods

In this section, we present the computational methods used in this paper which include machine learning methods, an empirical method, and a statistical method. The empirical method used in this paper adapts the USBM formula for predicting airblast. We utilised a total of 104 datasets obtained from the mine blasting records of the Orapa Diamond Mine owned by Debswana. Table 1 provides a summary of the input and output parameters considered in our analysis, with their corresponding minimum and maximum values. The input parameters listed in Table 1 were selected because they capture the key blast design and explosive factors influencing airblast in practical blasting operations. Burden and spacing, for example, reflect the confinement and distribution of the explosive load within the rock mass, directly affecting the pressure wave's intensity. Stemming length controls how gases and energy escape from the borehole, thereby influencing airblast levels. Hole depth and diameter relate to the total explosive volume and consequently how energy propagates through the rock, while the distance from the blast to the monitoring point determines how much the wave attenuates over distance. Linear charge and powder factor help characterise the explosive energy applied per unit length and volume, respectively, both of which strongly affect the overall vibration and airblast output. The methodology flow chart for the machine learning implementation stages is shown in Figure 2.

The process began with the collection of original data from the mine records. The collected data underwent a cleaning process to address inconsistencies and errors. Once cleaned, the data was then normalised to ensure that all input parameters were on a consistent scale and range. The dataset, after preprocessing, was divided into three parts: a training subset (80%), a validation subset (10%), and a testing subset (10%) as shown in Figure 2. The training subset was used to train the ML models, including, SVM, ANN, k-NN, and RF.

Performance indices like mean absolute error (MAE), R^2, and RMSE, were used to assess the trained models. These metrics assess how well the models can predict airblast values based on the input parameters. The models underwent a fine-tuning process, which involved adjusting their hyper-parameters to optimise their performance.

Figure 2 Flowchart for the machine learning model implementation stages

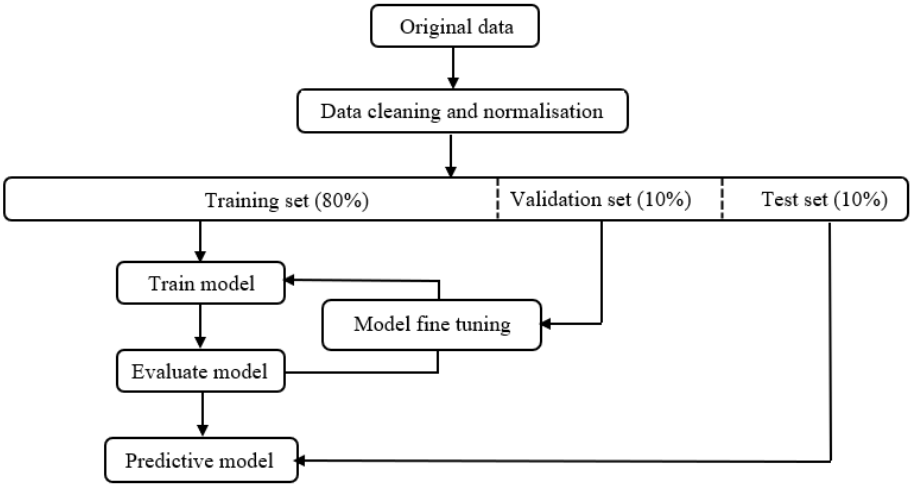

Figure 3 The RMSE values for different models, (a) RMSE for KNN model with different k (b) RMSE for RF model with different trees (c) RMSE for ANN model with different neurons (d) RMSE for SVM model with different sigma (see online version for colours)

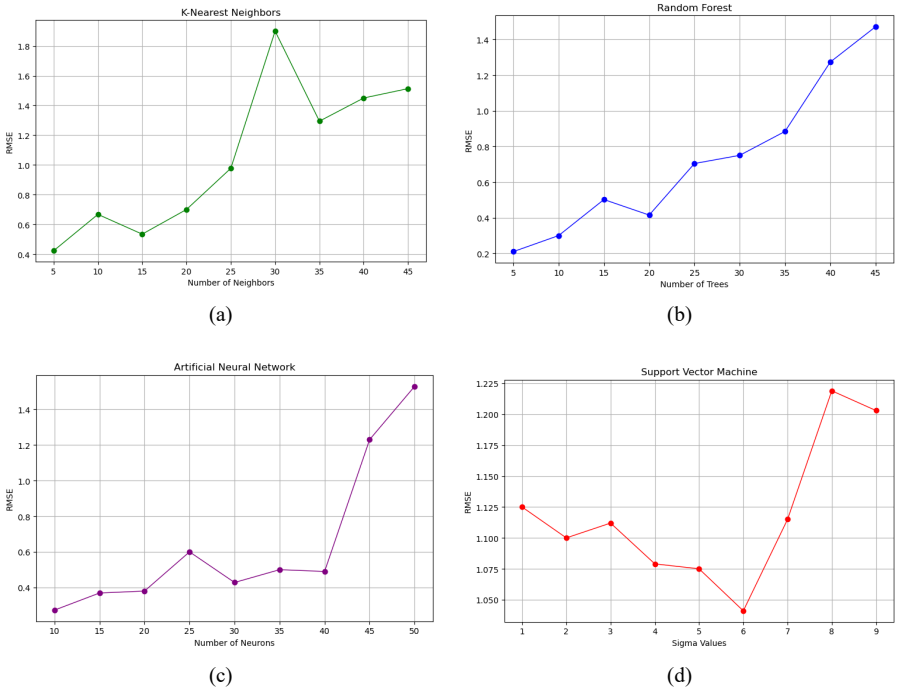

Figure 3 shows the variation in RMSE for different models with their hyper-parameters. Figure 3(a) shows the variation in the number of neighbours for the k-NN model with

RMSE. As the number of neighbours increases the RMSE increases, and the optimum model performance was found at k = 5 (lowest RMSE). For the RF model an increase in the number of trees, results in a higher RMSE, the optimum model was found at the number of trees = 5 (lowest RMSE) as shown in Figure 3(b). In Figure 3(c), the RMSE increases as the number of neurons increases with an optimum model being 10 neurons (lowest RMSE). For the SVM model, smaller and larger sigma values lead to a higher RMSE, while the medium values lead to a lower sigma value, with the optimum model being σ = 6. Once the models had been trained and evaluated, they were then used to make predictions on new, unseen data. These predictions provided estimates of airblast values based on the input parameters.

Table 1 Description of the input and output parameters for all models

Parameter	*Type*	*Unit*	*Symbol*	*Min*	*Max*
Burden	input	m	B	4	8
Spacing	input	m	S	5	9
Stemming length	input	m	T	4	6
Hole depth	input	m	L	12.3	15.2
Hole diameter	input	mm	D	165	250
Distance from blast to monitoring point	input	m	DI	438	1,500
Linear charge	input	kg/m	Lc	27	61.4
Powder factor	input	kg/m^3	Pf	0.3	1.2
Airblast	output	dB	Ab	91.5	126.7

2.1 Sensitivity analysis

Sensitivity analysis is typically conducted using the cosine amplitude method (Faradonbeh et al., 2016; Wang et al., 2023). Yang et al. (2014) applied the method for sensitivity analysis using network weights. The relative importance is calculated using (3):

$$I_j = \frac{\sum_{m=1}^{m=Nh} \frac{W_{jm}^{ih}}{\sum_{k=1}^{Ni} |W_{jm}^{ih}|} \times |W_{mn}^{ho}|}{\sum_{k=1}^{k=Ni} \sum_{m=1}^{m=Nh} \frac{|W_{jm}^{ih}|}{\sum_{k=1}^{Ni} |W_{km}^{ih}| \times |W_{mn}^{ho}|}} \tag{3}$$

In this context, I_j denotes the relative significance of the jth predictor in influencing the dependent variable; N_i and N_h correspond to the number of neurons within the input layer and the hidden layer, respectively; W represents the synaptic weight; where the superscript notations i, h, and o are indicative of the input, hidden, and output layers, correspondingly, and the subscript notations k, m and n are associated with the neuron indices in the input, hidden, and output layers, in that order.

2.2 Optimisation of blast parameters using gradient descent

This study employs gradient descent optimisation to find the minimum airblast value and its corresponding input parameters, which can be utilised by blast engineers in

their blast design. The Monte Carlo method was utilised to determine the optimal ANN model with eight inputs, one output, and two hidden layers, focusing on the optimal number of neurons in each hidden layer. The optimal ANN architecture is 8-80-10-1. The gradient descent technique was then used to navigate the solution space to find the minimum airblast and its corresponding optimised input parameters. Figure 4 shows the optimisation process. The gradient descent method is a widely used iterative optimisation technique that finds application in almost all areas of computation (Yang et al., 2014). The gradient descent technique is shown in (4):

$$p_i^{\text{new}} = p_i - \eta \left(\frac{\text{nnet}(p_1, \ldots, p_i, \ldots, p_N) - \text{nnet}(p_1, \ldots, p_i^{\text{old}}, \ldots, p_N)}{p_i - p_i^{\text{old}}} \right) \tag{4}$$

In this equation, p_i^{new} represents the updated parameter, while p_i is the current parameter value being updated. The term p_i^{old} denotes the parameter value from the previous iteration. The learning rate is represented as η. The function nnet represents the neural network model.

Figure 4 Flow chart for the gradient descent optimisation process (see online version for colours)

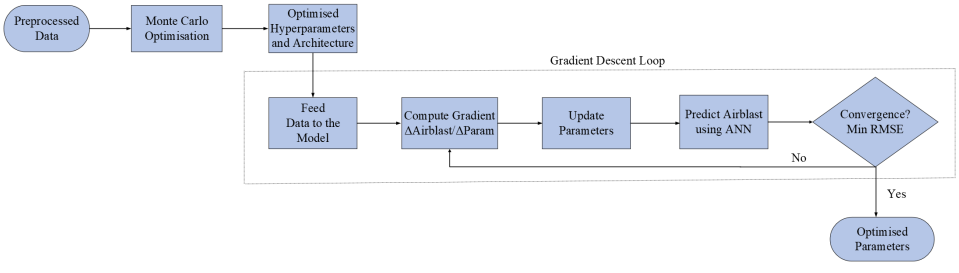

3 Results and discussion

The efficacy of each predictive model was evaluated using RMSE, MAE, and R^2 as performance metrics, as shown in equations (5) through (7) (Ikram et al., 2023; Ghazvinian et al., 2021):

$$RMSE = \sqrt{\frac{1}{n}\sum_{i=1}^{n}(y_i - y_i')^2} \tag{5}$$

$$MAE = \frac{1}{n}\sum_{i=1}^{n}|y_i - y_i'| \tag{6}$$

$$R^2 = \left[\frac{\sum_{i=1}^{n}(y_i - \bar{y}_i)(y_i' - \bar{y}_i')}{\sum_{i=1}^{n}(y_i - \bar{y}_i)^2 \sum_{i=1}^{n}(y_i' - \bar{y}_i')^2} \right]^2 \tag{7}$$

where n is the number of observations, y_i and y_i' are the measured and predicted values of the i^{th} observation, respectively; and $\bar{y}_i$ and $\bar{y}_i'$ are the mean values, respectively.

Table 2 The calculated performance indices for all algorithms

Method	R^2	*RMSE*	*MAE*
k-nearest neighbour			
n-neighbours = 5	0.945	1.037	0.330
n-neighbours = 15	0.639	1.188	0.324
n-neighbours = 25	0.524	1.677	0.385
n-neighbours = 35	0.546	1.894	0.361
n-neighbours = 45	0.769	2.013	1.046
Support vector machine			
sigma = 1	0.852	1.125	0.369
sigma = 3	0.863	1.112	0.389
sigma = 5	0.948	1.075	0.362
sigma = 7	0.872	1.115	0.467
sigma = 9	0.886	1.203	0.590
Random forest			
n-estimators = 5	0.955	0.210	0.322
n-estimators = 15	0.891	0.502	0.315
n-estimators = 25	0.885	0.704	0.344
n-estimators = 35	0.894	0.884	0.478
n-estimators = 45	0.785	1.471	0.682
Artificial neural network			
model 1 (10 neurons)	0.988	0.273	0.189
model 2 (20 neurons)	0.918	0.380	0.261
model 3 (30 neurons)	0.894	0.428	0.265
model 4 (40 neurons)	0.889	0.490	0.387
model 5 (50 neurons)	0.862	1.529	0.390
Multivariant regression model			
regression model	0.485	2.363	1.490
Empirical model (USMB)			
empirical model	0.149	11.034	9.232

The results of the calculated performance indices of the test set for all models are summarised in Table 2. Based on the performance indices presented in Table 2, it is evident that the ANN model with an architecture of 8-10-1 (eight inputs, ten neurons in the hidden layer, one output) exhibits the lowest RMSE (0.273), lowest MAE (0.189), and the highest R^2 (0.988). In contrast, the empirical model USBM demonstrates poor prediction capabilities with RMSE, MAE, and R^2 values of 11.034, 9.232, and 0.149, respectively. Therefore, the ANN 8-10-1 model is considered to be the optimum model for predicting airblast.

Figures 6(a) to 6(d) depict the correlations between the measured and predicted airblast values for all the machine learning models. The data points closely align with the line of best fit for the ANN model, illustrating the high correlation and improved prediction capability of the ANN compared to other models. In contrast, Figures 6(e) and 6(f) indicate that the data points for the MVRA and USBM models deviate significantly from the line of best fit, indicating poor correlation and limited prediction capabilities.

Table 3 Performance indices from other machine learning studies related to airblast

Best model	*Other models*	*Inputs*	*Dataset*	R^2	*Reference*
ANN	MVRA, Generalised equation	DI, MC	56	0.96	Khandelwal and Singh (2005)
SVM	Generalised equation	DI, MC	75	0.85	Khandelwal and Kankar (2011)
ANN	FIS	DI, MC	162	0.92	Mohamed (2011)
ANN	-	D, S, B, N, D, T, Pf	38	0.93	Mohamad et al. (2012)
PSO-ANN	USBM, NAAS, Mckenzine	D, S, B, T, Pf, N, DI, C, RQD	62	0.86	Hajihassani et al. (2014)
ICA-ANN	-	DI, MC	70	0.96	Armaghani et al. (2016)
GA-ANN	ANN, USBM, MVRA	DI, MC	97	0.96	Armaghani et al. (2018)
BPNN	BRNN, MLPNN, ANFIS	Q, H, B, S, T, Pf, N	146	0.96	Nguyen et al. (2020)
RF-ANN	ANN, RF, USBM	Q, DI, H, Pf, B, S, T	114	0.98	Nguyen and Bui (2019)
SVM-GO-BFS	SVM	RQD, B, D, S, Pf, T	62	0.98	Chen et al. (2022)
FCM-UIM	BPCWNN, BPNN, GFFNN	N, B, S, H/B, T, PF, Q, DI	90	0.98	Hosseini et al. (2022b)
ANN-KNN	ANN, USBM	MC, DI	75	0.90	Amiri et al. (2016)
RBF-ANN	RF, SVM, MLP, GA-MLP, MARS	D, T, B, S, MC, Pf, DI	76	0.95	Zhang et al. (2022)
XGBoost	RF, ANN, SVM, KNN	T, Pf, DI, MC	62	0.86	He et al. (2021)
ANN	USBM, Indian Standard, MVRA	MC, DI, D, T, S/B D, Pf	180	0.99	Tiile (2016)

Note: USBM, US Bureau of Mines; NAAS, National Association of Australian State; MLR, multi-linear regression; MCFR, modified conjugate Fletcher and Reeves method; BRNN, bidirectional recurrent neural network; MLPNN, multi-layer perceptron neural network; FIS, fuzzy inference system; ANFIS, adaptive neuro fuzzy inference system; FCM-UIM, fuzzy cognitive map-uncertainty intelligence method; H, bench height; Q, charge per delay; Sd, subdrill; TC, total charge; DI, distance; S/B, spacing to burden ratio; N, number of holes; MC, maximum charge per delay; RQD, rock quality designation; MARS, multi-adaptive regression spline; XGBoost, extreme gradient boosting.

Figure 5 Scatter plots for all the models, (a) ANN 8-10-1 model performance (b) SVM (sigma = 5) model performance (c) *k*-NN (5) model performance (d) RF (no. trees = 5) model performance (e) MVRA model performance (f) USBM model performance (see online version for colours)

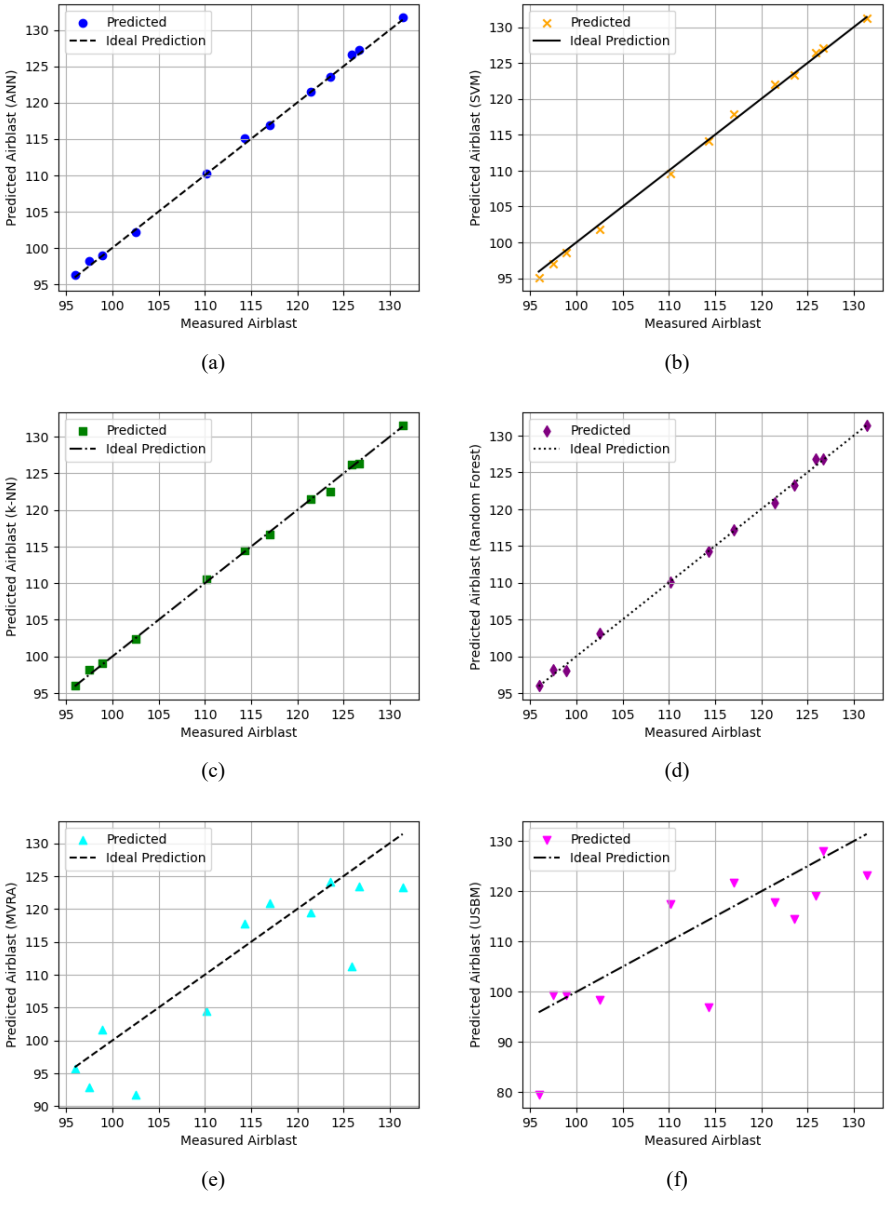

The ANN excels due to its ability to handle nonlinear relationships through its adaptive and flexible structure. Unlike traditional machine learning models, ANN can automatically learn complex patterns directly from data without relying on predefined assumptions. Their interconnected neurons and multiple layers allow them to model intricate relationships, while activation functions introduce nonlinearity, enabling

them to approximate complex functions. Additionally, optimisation techniques like backpropagation ensure effective learning, making ANN particularly suitable for tasks with high-dimensional data and complex patterns, thus outperforming other models.

Figure 6 Sensitivity analysis of airblast (see online version for colours)

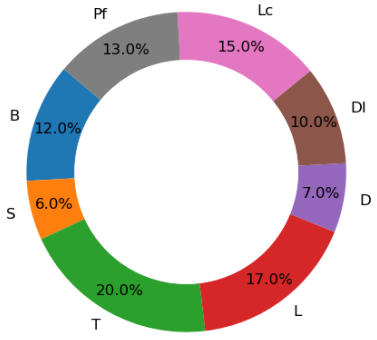

The k-NN model (R^2 = 0.945, RMSE = 1.037) may perform this way because it assumes that similar inputs yield similar outputs, which might not hold if there is insufficient local similarity for predicting blast-induced airblast. Moreover, for high-dimensional datasets like ours, the "curse of dimensionality" can limit KNN's ability to identify meaningful neighbours. The SVM model (R^2 = 0.948, RMSE = 1.075) relies heavily on careful tuning of multiple hyperparameters such as (kernel type, regularisation, and margin), so slight deviations from optimal settings can degrade its performance, especially when capturing highly nonlinear patterns in the data. The random forest model achieved a relatively higher R^2 of 0.955 and an RMSE of 0.210. However, its ensemble-based approach typically benefits most from larger, more diverse datasets, where multiple subsets can be drawn to produce robust decision trees. The MVRA model, which is a traditional linear approach, fails to capture nonlinear relationships. The USBM formula performs poorly because, like MVRA, it relies on linear assumptions and cannot accurately represent the complex nonlinear nature of airblast data, making it the least effective model.

The highest-performing model in Table 3 is the ANN model by Tiile (2016), which achieved an R^2 of 0.99 using 180 blasting events with seven inputs (maximum charge per delay (MC), DI, D, T, S/B, D, Pf). This model's superior performance can be attributed to the large dataset size and more inputs. In contrast, the lowest-performing model is the SVM model by Khandelwal and Kankar (2011) with an R^2 of 0.85 using 75 blasting events and two inputs (MC, DI). The smaller dataset size, few inputs, and potential challenges with hyperparameter tuning of the SVM model might have restricted the model's ability to generalize and capture the variability in the data, leading to lower predictive accuracy. In the middle range, the ANN-KNN by Amiri et al. (2016) achieved an R^2 of 0.90 using 75 datasets with two inputs (DI, MC). This model combines the k-NN algorithm with ANN, enabling it to handle larger and more diverse datasets effectively. Its performance is better than the lowest-performing model, indicating that hybrid techniques can significantly enhance predictive capabilities. Our ANN model achieved an R^2 of 0.988 with 100 datasets and eight inputs. It performs well and aligns

closely with other high-performing models, such as the SVM-GO-BFS by Chen et al. (2022), which achieved an R^2 of 0.98 with 62 blasting events and six inputs.

Figure 7 Solution space for airblast as the output parameter with eight input parameters, taken two at a time (see online version for colours)

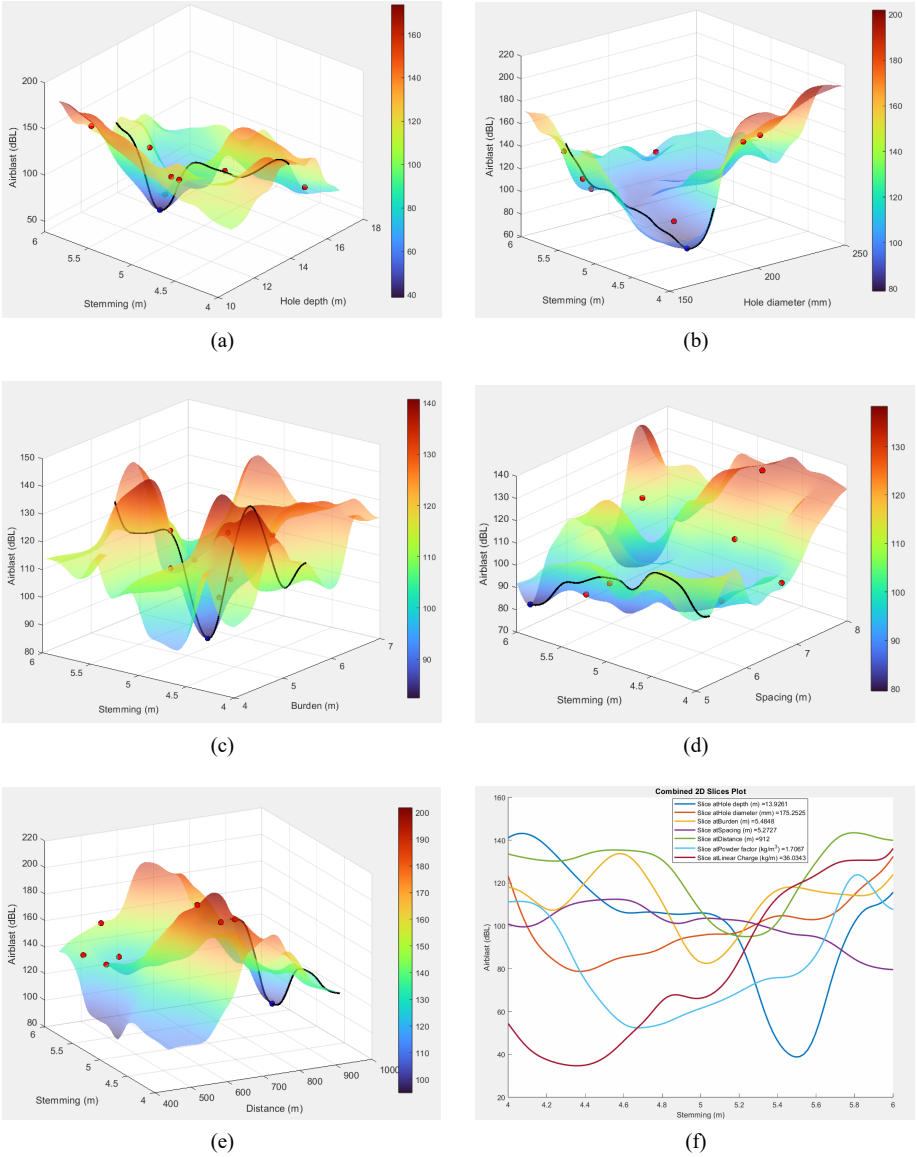

Note: The red dots are random initial values that always converge to the optimal point, the blue dot, for every minimisation computation. Airblast versus stemming, the most influential input parameter, presented in a 2D plot. The values of the other seven input parameters at the optimal point are kept constant, while stemming is plotted in its entire range.

Our ANN model performed well compared to the hybrid models (PSO-ANN, ICA-ANN, and XGBoost), all of which used fewer inputs and smaller datasets than our model. Additionally, our ANN achieved slightly better performance (R^2 = 98.8%) than the RF-ANN model (R^2 = 98%), which utilised the same number of inputs but had a slightly larger dataset. These results imply that the accuracy and generalisability of a model can be improved by investigating hybrid models and increasing dataset size, this allows the model to capture more complex interactions and improve generalisability, as seen in the highest-performing models.

3.1 Sensitivity analysis

From Figure 6, it can be inferred that stemming (T) is the most influential input parameter on airblast with 20%. It is also noted that the level of airblast is least sensitive to the spacing (S) with 6%. The sensitivity analysis highlights the critical role of stemming in influencing airblast. These parameters should be given priority during the blast design process. The high sensitivity of stemming suggests that even minor adjustments can lead to significant changes in airblast levels, providing a powerful lever for engineers to control blast outcomes. On the other hand, the relatively low sensitivity of spacing indicates that it can be considered a secondary factor, allowing engineers to focus their optimisation efforts on more influential parameters.

Building on the sensitivity analysis that identified stemming as the most influential parameter for airblast control, practical implementation starts with small-scale trials to determine the optimal stemming length for each site's geological conditions. Carefully selecting a suitable stemming material such as a denser, more cohesive aggregate further enhances explosive gas containment, and this choice should be balanced through a cost-benefit analysis to ensure operational feasibility. Incorporating real-time airblast measurements will allow for continual refinement of stemming parameters across successive blasts. While stemming plays a critical role, it is nonetheless important to integrate these adjustments with other design variables like burden, hole diameter, and spacing to maintain overall blast efficiency, safety, and effectiveness.

3.2 Optimisation of airblast

Figures 7(a) through 7(e) display the results of the optimisation procedure, starting with seven initial points (depicted as red dots) chosen at random and converging towards the optimal value (illustrated as a blue dot), which is the lowest point in the surface. The optimal solution is consistent throughout all random initial points and has a value of around 40 dB. Each curve plotted in subfigures is one of the seven input parameters. Subfigures shows a 3D plot where stemming, the second most influential parameter, is kept constant in the traced curve that includes the blue dot which is the minimum point. The red dots are random initial points converging to the blue dot at every optimisation computation. The optimised blast design parameters are as follows: powder factor (1.15), linear charge (42), burden (5.5), spacing (5.5), stemming (6), distance from blast point to monitoring point (980), hole depth (14), and diameter (170). Every point in the solution surface has nine components, i.e., eight components of the eight input parameters plus the output component of the airblast. From the sensitivity analysis, stemming is the most influential parameter. Because of this, we compare stemming versus all the other seven

input parameters kept constant, to observe the variations in the values of the output parameter in a two-dimensional plot. We assign stemming to be the x-axis, while airblast is assigned as the y-axis.

In Figure 7(a), when stemming decreases while hole depth is fixed, airblast initially decreases towards an optimal stemming value that minimises airblast and rises again. Figure 7(b) shows that as stemming decreases with the hole diameter fixed, airblast gradually decreases towards an optimal stemming value for minimal airblast and then increases. In Figure 7(c), decreasing stemming while keeping the burden fixed results in a sharp decrease in airblast to an optimal value, and then it rises again. Figure 7(d) demonstrates that with spacing fixed, airblast gradually decreases with an increase in stemming up to the lowest optimal point. Figure 7(e) shows with the distance from the blast point to the monitoring point kept constant, airblast decreases to an optimal point as stemming increases, after which it begins to rise.

The solution space also confirms the results of the sensitivity analysis. As can be seen in Figure 7(f), generated by varying stemming and fixing all the other parameters, and taking a slice through the lowest, optimised point in the solution space. Hole depth is the second most influential input parameter after stemming, and has the largest variation ranging from about 39–142 dB in Figure 7(f). This indicates a high sensitivity, as changes in hole depth significantly impact airblast. Spacing is the least influential parameter, this parameter shows variations from about 80–110 dB, also suggesting lower sensitivity.

The significance of these results lies in their practical application for blasting engineers seeking to minimise the environmental and structural impacts of airblast during blasting operations. By providing a set of optimised parameters, the model enables engineers to design blasts that adhere to safety regulations and reduce the risk of noise and pressure wave damage to nearby structures and communities. Reducing airblast mitigates the risk of structural damage and enhances the blasting process' efficiency. Minimising airblast can lead to more controlled and precise rock fragmentation, potentially reducing the need for secondary blasting and lowering operational costs.

4 Conclusions

This study shows a method for modelling airblast using machine learning in an open-pit mine located in Orapa, Botswana owned by Debswana Diamond Company. We employed four machine learning algorithms, namely, ANN, SVM, RF, and k-NN. The USBM empirical formula and the MVRA statistical method are used to compare results against the machine learning models. The sensitivity analysis is performed to determine the most influential parameter out of the eight input parameters. The most influential input parameter on airblast is stemming (T). Conversely, the spacing (S) showed the least sensitivity to airblast. Of all the machine learning models, the ANN model is the best-performing one. This model is then optimised in terms of its architecture for the number of neurons in each of the two hidden layers. Using the optimised machine learning model, the minimum airblast was calculated to be approximately 40 dB using the gradient descent technique. The values of its corresponding input parameters are powder factor (1.15), charge (42), burden (5.5), spacing (5.5), stemming (6), distance from the blast point to the monitoring point (980), hole depth (14), and hole diameter

(170). The study's findings apply to Orapa diamond mine, but its scalable methodology can be adapted to other mines by incorporating site-specific data and retraining the model for varying geological, topographical, and operational conditions.

References

Abdalla, A. and Salih, A. (2022) 'Implementation of multi-expression programming (MEP), artificial neural network (ANN), and M5P-tree to forecast the compression strength cement-based mortar modified by calcium hydroxide at different mix proportions and curing ages', *Innovative Infrastructure Solutions*, Vol. 7, No. 2, p.153.

Amiri, M., Amnieh, H.B., Hasanipanah, M. and Khanli, L.M. (2016) 'A new combination of artificial neural network and k-nearest neighbors models to predict blast-induced ground vibration and air-overpressure', *Engineering with Computers*, Vol. 32, pp.631–644.

Armaghani, D.J., Hajihassani, M., Marto, A., Faradonbeh, R.S. and Mohamad, E.T. (2015a) 'Prediction of blast-induced air overpressure: a hybrid AI-based predictive model', *Environmental Monitoring and Assessment*, Vol. 187, No. 11, pp.1–13.

Armaghani, D.J., Hajihassani, M., Sohaei, H., Mohamad, E.T., Marto, A., Motaghedi, H. and Moghaddam, M.R. (2015b) 'Neuro-fuzzy technique to predict air-overpressure induced by blasting', *Arabian Journal of Geosciences*, Vol. 8, No. 12, pp.10937–10950.

Armaghani, D.J., Hasanipanah, M., Mahdiyar, A., Abd Majid, M.Z., Amnieh, H.B. and Tahir, M. (2018) 'Airblast prediction through a hybrid genetic algorithm-ANN model', *Neural Computing and Applications*, Vol. 29, No. 9, pp.619–629.

Armaghani, D.J., Hasanipanah, M. and Mohamad, E.T. (2016) 'A combination of the ICA-ANN model to predict air-overpressure resulting from blasting', *Engineering with Computers*, Vol. 32, No. 1, pp.155–171.

Armaghani, D.J., Ming, Y.Y., Mohammed, A.S., Momeni, E. and Maizir, H. (2023) 'Effect of SVM kernel functions on bearing capacity assessment of deep foundations', *Journal of Soft Computing in Civil Engineering*, Vol. 7, No. 3, pp.111–128.

Bakhtavar, E., Hosseini, S., Hewage, K. and Sadiq, R. (2021) 'Green blasting policy: simultaneous forecast of vertical and horizontal distribution of dust emissions using artificial causality-weighted neural network', *Journal of Cleaner Production*, Vol. 283, No. 1, p.124562.

Bhandari, S. (1997) *Engineering Rock Blasting Operations*, A.A. Balkema, Netherlands, ISBN: 978-90-5410-663-0.

Cai, M., Hocine, O., Mohammed, A.S., Chen, X., Amar, M.N. and Hasanipanah, M. (2022) 'Integrating the LSSVM and RBFNN models with three optimization algorithms to predict the soil liquefaction potential', *Engineering with Computers*, Vol. 38, No. 4, pp.3611–3623.

Chen, L., Asteris, P.G., Tsoukalas, M.Z., Armaghani, D.J., Ulrikh, D.V. and Yari, M. (2022) 'Forecast of airblast vibrations induced by blasting using support vector regression optimized by the grasshopper optimization (SVR-GO) technique', *Applied Sciences*, Vol. 12, No. 19, p.9805.

Dindarloo, S. (2015) 'Peak particle velocity prediction using support vector machines: a surface blasting case study', *Journal of the Southern African Institute of Mining and Metallurgy*, Vol. 115, No. 7, pp.637–643.

Dumakor-Dupey, N.K., Arya, S. and Jha, A. (2021) 'Advances in blast-induced impact prediction – a review of machine learning applications', *Minerals*, Vol. 11, No. 6, p.601.

Faradonbeh, R.S., Monjezi, M. and Armaghani, D.J. (2016) 'Genetic programing and non-linear multiple regression techniques to predict backbreak in blasting operation', *Engineering with Computers*, Vol. 32, No. 1, pp.123–133.

Faramarzi, F., Farsangi, M.A.E. and Mansouri, H. (2014) 'Simultaneous investigation of blast induced ground vibration and airblast effects on safety level of structures and human in surface blasting', *International Journal of Mining Science and Technology*, Vol. 24, No. 5, pp.663–669.

Gaopale, K., Jamisola, R.S. and Seitshiro, I. (2019) *Application of Artificial Neural Networks to Predict Blast-Induced Ground Vibration in a Diamond Mine*.

Ghazvinian, H., Karami, H., Farzin, S. and Mousavi, S-F. (2021) 'Introducing affordable and accessible physical covers to reduce evaporation from agricultural water reservoirs and pools (field study, statistics, and intelligent methods)', *Arabian Journal of Geosciences*, Vol. 14, No. 23, pp.1–28.

Hajihassani, M., Armaghani, D.J., Sohaei, H., Mohamad, E.T. and Marto, A. (2014) 'Prediction of airblast-overpressure induced by blasting using a hybrid artificial neural network and particle swarm optimization', *Applied Acoustics*, Vol. 80, No. 1, pp.57–67.

He, Z., Armaghani, D.J., Masoumnezhad, M., Khandelwal, M., Zhou, J. and Murlidhar, B.R. (2021) 'A combination of expert-based system and advanced decision-tree algorithms to predict air-overpressure resulting from quarry blasting', *Natural Resources Research*, Vol. 30, No. 5, pp.1889–1903.

Hosseini, S., Mousavi, A., Monjezi, M. and Khandelwal, M. (2022a) 'Mine-to-crusher policy: planning of mine blasting patterns for environmentally friendly and optimum fragmentation using Monte Carlo simulation-based multi-objective grey wolf optimization approach', *Resources Policy*, Vol. 79, No. Part C, p.103087.

Hosseini, S., Poormirzaee, R. and Hajihassani, M. (2022b) 'Application of reliability-based back-propagation causality-weighted neural networks to estimate air-overpressure due to mine blasting', *Engineering Applications of Artificial Intelligence*, Vol. 115, p.105281.

Hosseini, S., Poormirzaee, R. and Hajihassani, M. (2022c) 'An uncertainty hybrid model for risk assessment and prediction of blast-induced rock mass fragmentation', *International Journal of Rock Mechanics and Mining Sciences*, Vol. 160, p.105250.

Hustrulid, W. (1999) *Blasting Principles for Open Pit Mining: Volume 2 – Theoretical Foundations*, AA Balkema.

Ikram, R.M.A., Mostafa, R.R., Chen, Z., Parmar, K.S., Kisi, O. and Zounemat-Kermani, M. (2023) 'Water temperature prediction using improved deep learning methods through reptile search algorithm and weighted mean of vectors optimizer', *Journal of Marine Science and Engineering*, Vol. 11, No. 2, p.259.

Kaklis, K., Saubi, O., Jamisola, R. and Agioutantis, Z. (2022) 'Machine learning prediction of the load evolution in three-point bending tests of marble', *Mining, Metallurgy & Exploration*, Vol. 39, No. 5, pp.2037–2045.

Keshtegar, B., Hasanipanah, M., Bakhshayeshi, I. and Sarafraz, M.E. (2019) 'A novel nonlinear modeling for the prediction of blast-induced airblast using a modified conjugate FR method', *Measurement*, Vol. 131, pp.35–41.

Khandelwal, M. and Kankar, P. (2011) 'Prediction of blast-induced air overpressure using support vector machine', *Arabian Journal of Geosciences*, Vol. 4, No. 3, pp.427–433.

Khandelwal, M. and Singh, T. (2005) 'Prediction of blast induced air overpressure in opencast mine', *Noise & Vibration Worldwide*, Vol. 36, No. 2, pp.7–16.

Kuzu, C., Fisne, A. and Ercelebi, S. (2009) 'Operational and geological parameters in the assessing blast induced airblast-overpressure in quarries', *Applied Acoustics*, Vol. 70, No. 3, pp.404–411.

Le, L.T., Nguyen, H., Dou, J. and Zhou, J. (2019) 'A comparative study of PSO-ANN, GA-ANN, ICA-ANN, and ABC-ANN in estimating the heating load of buildings' energy efficiency for smart city planning', *Applied Sciences*, Vol. 9, No. 13, p.2630.

Mahdiyar, A., Marto, A. and Mirhosseinei, S.A. (2018) 'Probabilistic air-overpressure simulation resulting from blasting operations', *Environmental Earth Sciences*, Vol. 77, No. 4, pp.1–11.

Mahmood, W. and Mohammed, A. (2022) 'Performance of ANN and M5P-tree to forecast the compressive strength of hand-mix cement-grouted sands modified with polymer using ASTM and BS standards and evaluate the outcomes using SI with OBJ assessments', *Neural Computing and Applications*, Vol. 34, No. 17, pp.15031–15051.

Mohamad, E.T., Armaghani, D.J., Hasanipanah, M., Murlidhar, B.R. and Alel, M.N.A. (2016) 'Estimation of air-overpressure produced by blasting operation through a neuro-genetic technique', *Environmental Earth Sciences*, Vol. 75, No. 2, pp.1–15.

Mohamad, E.T., Hajihassani, M., Armaghani, D.J. and Marto, A. (2012) 'Simulation of blasting-induced air overpressure by means of artificial neural networks', *Int Rev Model Simul*, Vol. 5, No. 6, pp.2501–2506.

Mohamed, M.T. (2011) 'Performance of fuzzy logic and artificial neural network in prediction of ground and air vibrations', *JES. Journal of Engineering Sciences*, Vol. 39, No. 2, pp.425–440.

Monjezi, M. and Dehghani, H. (2008) 'Evaluation of effect of blasting pattern parameters on back break using neural networks', *International Journal of Rock Mechanics and Mining Sciences*, Vol. 45, No. 8, pp.1446–1453.

Nguyen, H. and Bui, X-N. (2019) 'Predicting blast-induced air overpressure: a robust artificial intelligence system based on artificial neural networks and random forest', *Natural Resources Research*, Vol. 28, No. 3, pp.893–907.

Nguyen, H. and Bui, X-N. (2020) 'Soft computing models for predicting blast-induced air over-pressure: a novel artificial intelligence approach', *Applied Soft Computing*, Vol. 92, p.106292.

Nguyen, H., Bui, X-N., Bui, H-B. and Mai, N-L. (2020) 'A comparative study of artificial neural networks in predicting blast-induced air-blast overpressure at Deo Nai open-pit coal mine, Vietnam', *Neural Computing and Applications*, Vol. 32, No. 8, pp.3939–3955.

Saubi, O., Gaopale, K., Jamisola, R., Suglo, R., Matsebe, O. et al. (2023a) 'Prediction of blast-induced rock fragmentation at Orapa Diamond Mine using hybrid ANN models', *Proceedings of the 2023 Teaching and Research in Data Analytics and Information Systems (TRDAIS) Conference*, Palapye, Botswana.

Saubi, O., Gaopale, K., Jamisola, R.S., Suglo, R.S. and Matsebe, O. (2023b) 'Enhancing blast design efficiency for rock fragmentation with gradient descent and artificial neural networks: an optimization study', *2023 4th International Conference on Computers and Artificial Intelligence Technology (CAIT)*, IEEE, pp.1–5.

Sawmliana, C., Roy, P.P., Singh, R. and Singh, T. (2007) 'Blast induced air overpressure and its prediction using artificial neural network', *Mining Technology*, Vol. 116, No. 2, pp.41–48.

Singh, T., Kanchan, R. and Verma, A. (2004) 'Prediction of blast induced ground vibration and frequency using an artificial intelligent technique', *Noise & Vibration Worldwide*, Vol. 35, No. 11, pp.7–15.

Siskind, D.E., Strachura, V., Stagg, M.S. and Kopp, J.W. (1980) *Structure Response and Damage Produced by Airblast from Surface Mining*, Vol. 8485, US Department of the Interior, Bureau of Mines, Washington, DC.

Temeng, V.A., Ziggah, Y.Y. and Arthur, C.K. (2020) 'A novel artificial intelligent model for predicting air overpressure using brain inspired emotional neural network', *International Journal of Mining Science and Technology*, Vol. 30, No. 5, pp.683–689.

Tiile, R.N. (2016) *Artificial Neural Network Approach to Predict Blast-Induced Ground Vibration, Airblast and Rock Fragmentation*, Master's thesis, Missouri University of Science and Technology.

Trivedi, R., Singh, T. and Gupta, N. (2015) 'Prediction of blast-induced flyrock in opencast mines using ANN and ANFIS', *Geotechnical and Geological Engineering*, Vol. 33, No. 4, pp.875–891.

Wang, X., Hosseini, S., Armaghani, D.J. and Mohamad, E.T. (2023) 'Data-driven optimized artificial neural network technique for prediction of flyrock induced by boulder blasting', *Mathematics*, Vol. 11, No. 10, p.2358.

Yang, Y., Lin, X., Wei, B., Zhao, Y. and Wang, J. (2014) 'Evaluation of adsorption potential of bamboo biochar for metal-complex dye: equilibrium, kinetics and artificial neural network modeling', *International Journal of Environmental Science and Technology*, Vol. 11, No. 4, pp.1093–1100.

Yu, Z., Shi, X., Zhou, J., Chen, X. and Qiu, X. (2020) 'Effective assessment of blast-induced ground vibration using an optimized random forest model based on a Harris hawks optimization algorithm', *Applied Sciences*, Vol. 10, No. 4, p.1403.

Zeng, J., Roussis, P.C., Mohammed, A.S., Maraveas, C., Fatemi, S.A., Armaghani, D.J. and Asteris, P.G. (2021) 'Prediction of peak particle velocity caused by blasting through the combinations of boosted-chaid and SVM models with various kernels', *Applied Sciences*, Vol. 11, No. 8, p.3705.

Zhang, R., Li, Y., Gui, Y. and Zhou, J. (2022) 'Prediction of blasting induced air-overpressure using a radial basis function network with an additional hidden layer', *Applied Soft Computing*, Vol. 127, No. Part C, p.109343.